# Synthesis and Characterization Ni/Fe-MOF and Its **Performance for Supercapacitor Application**

Hakim Habibi<sup>1,3</sup>, Brian Yulianto<sup>2</sup>, Muhammad Iqbal<sup>2</sup>, N. L. Wulan Septiani<sup>24</sup>, & N. Astri Lidiawati<sup>2</sup>

<sup>1</sup> Master Program of Engineering Physics, Institut Teknologi Bandung, Bandung 40132, Indonesia

<sup>2</sup> Advanced Functional Materials Laboratory, Faculty of Industrial Technology, Institut Teknologi Bandung, Bandung 40132, Indonesia

<sup>3</sup>PT Perusahaan Listrik Negara (Persero) Puslitbang, Jakarta 12760, Indonesia <sup>4</sup>Research Center for Nanotechnology System, National Research and Innovation Agency, South Tangerang 15314, Indonesia

Email: hakim.habibi@pln.co.id

Abstract. Metal-organic frameworks (MOFs) are widely used for supercapacitor electrodes due to their large surface area, high porosity, and adaptability. However, the low conductivity of pure MOFs limits their application as electrode materials. Various techniques are employed to overcome this, including creating bimetallic MOFs or making a composite. This study focuses on the novel bimetallic Ni/Fe-MOF, comparing its characteristics to Ni-MOF. The synthesis of MOFs is achieved using a single-step solvothermal method at 150 °C for 48 h, using terephthalic acid (BDC) as ligans. For solvent, ethylene glycol is added as a capping agent. Ni/Fe-MOF exhibits high capacitive properties, with a specific capacitance of 688 Fg<sup>-1</sup> at 0.5 Ag<sup>-1</sup>. Both have almost the same Flake-like morphology. These findings suggest that bimetallic Ni/Fe-MOF using solvothermal are promising candidates for improving Ni-MOF performance as supercapacitor electrodes, potentially advancing energy storage technology.

**Keywords:** supercapacitor, MOFs, energy storage.

#### 1 Introduction

The growing need for efficient and sustainable energy storage solutions has driven significant research into advanced electrochemical devices such as supercapacitors, Abbas, et al in [1]. Supercapacitors are known for their high power density, fast power charge/discharge rates, and good cyclic perfomance. It's ideal for energy storage applications requiring quick bursts of power, such as switching in power systems, Navarro, et al in [2]. However, their performance heavily depends on the electrode materials used.

Metal-organic frameworks (MOFs) have recently gained attention as promising materials for supercapacitor electrodes. MOFs are made from metal nodes and organic linkers, forming porous structures with large surface areas and tunable

, Accepted for publication

pore sizes. Moreover, redox-active metal centers within MOFs can improve their electrochemical performance, Khan *et al.* in [3]. However, despite these advantages, pure MOFs often need better electrical conductivity and stability, limiting their direct use in energy storage devices such as supercapacitors.

To overcome these limitations, some strategies include incorporating additional metal ions into MOF structures to create bimetallic MOFs or forming composite materials. Bimetallic MOFs, which contain two different metal ions within their framework, offer improved conductivity, stability, and capacitance compared to their single-metal counterparts. Bimetallic MOFs benefit from synergistic effects between the two metal centers by introducing a second metal ion, enhancing the overall electrochemical properties, Raza, *et al* in [4].

This study focuses on a novel bimetallic Ni/Fe-MOF, synthesized using a solvothermal method, which addresses the conductivity and stability challenges associated with pure MOFs. By partially replacing Ni<sup>2+</sup> with Fe<sup>2+</sup>, the resulting Ni/Fe-MOF offers improved electrochemical performance while maintaining the structural advantages of MOFs. This work aims to advance the development of high-performance supercapacitor electrodes by demonstrating the potential of bimetallic MOFs to enhance capacitance, contributing to the broader field of energy storage technology.

## 2 Experimental Section

#### 2.1 Materials

The precursor materials involved include terephthalic acid (BDC, purity 98%), Nickel(II) nitrate hexahydrate (Ni(NO<sub>3</sub>)<sub>2</sub>.6H<sub>2</sub>O, purity  $\geq$  98.5%), Cobalt(II) Nitrate Hexahydrate (Co(NO<sub>3</sub>)<sub>2</sub>.6H<sub>2</sub>O, purity  $\geq$  98%), Iron(III) nitrate nonahydrate (Fe(NO<sub>3</sub>)<sub>3</sub>.9H2O, purity  $\geq$  98%) from Sigma Aldrich, and Manganese(II) Nitrate Hydrate (Mn(NO<sub>3</sub>)<sub>2</sub>.4H<sub>2</sub>O, purity  $\geq$  98.5%) from Supelco. The solvents utilized in the process are dimethylformamide (DMF), ethanol, deionized water, and ethylene glycol. All chemical reagents utilized were of analytical quality and did not undergo any further refinement.

## 2.2 Synthesis of Ni-MOF and Ni/Fe-MOF

The method for synthesizing Ni-MOF used in this research emulates the established proses in a previous related study by Nie et al. [5], with ethylene glycol as an additional solvent. A mixture of 0.083 g of BDC and 0.145 g of Ni(NO<sub>3</sub>)<sub>2</sub>.6H<sub>2</sub>O was added to a solvent mixture consisting of 11 mL of DMF, 6 mL of ethanol, 5 mL of ethylene glycol, and 6 mL of deionized water. The mix was then stirred and sonicated to accelerate the dissolution process. The solution

was then moved to a Teflon-lined autoclave and subjected to a temperature of 150°C for a duration of 48 hours. The resulting samples were separated through centrifugation and purified with ethanol. Finally, the samples were dried at 60°C to produce Ni-MOF.

Meanwhile, the synthesizing of Ni/Fe-MOF was using the same method but with a small difference in the precursor. For Ni/Fe-MOF, 0.145 g of Ni(NO<sub>3</sub>)<sub>2</sub>.6H<sub>2</sub>O was replaced with 0.073 g of Ni(NO<sub>3</sub>)<sub>2</sub>.6H<sub>2</sub>O and 0.063 g of Fe(NO<sub>3</sub>)<sub>2</sub>.4H<sub>2</sub>O.

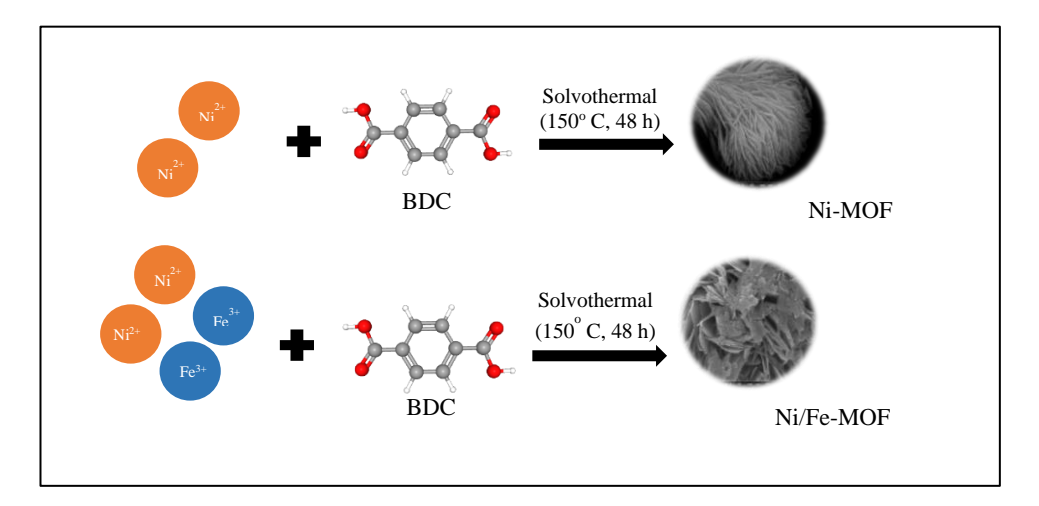


**Figure 1** The illustration of the syntesis process of Ni-MOF and Ni/Fe-MOF using BDC as ligan.

## 2.3 Materials characterization

Scanning electron microscopy (Foto Thermoscienrific: Quanta 650) was used to discover the morphology of the materials. Meanwhile, the crystallization was observed using X-ray diffraction (XRD) Rigaku minifies. Moreover, Fourier transform infrared (FTIR) analysis of the samples was conducted using an FTIR spectrometer (FTIR Prestige 21, Shimadzu) over the wavenumber range of 400–4000 cm<sup>-1</sup>.

#### 2.4 Electrochemical measurements

The properties of MOF electrode materials were tested using a three-electrode system in a 2.0 M KOH electrolyte with a CHI instrument and electrochemical workstation. The working electrode used the fabricated materials, and the counter electrode used a platinum wire, and as the reference using Ag/AgCl. Before the main testing, several CV tests were conducted to ensure the stability of the curve. Afterward, the polarization curve was obtained at a scan rate of 5, 10, 20, 40, 60,

80 and 100 mV s<sup>-1</sup>. GCD was conducted at 0.5, 1, 2, and 4  $Ag^{-1}$ . The specific capacitance (F  $g^{-1}$ ) was obtained using Eq. (1).

$$C = \frac{I \times \Delta t}{m \Delta V} \tag{1}$$

Where C (F g<sup>-1</sup>), I (A),  $\Delta t$  (s), m (g), and  $\Delta V$  (V) are specific capacity, discharge current and time, a mass of active material, and potential window, respectively.

#### 3 Results and discussion

SEM was conducted to illustrate the surface morphologies of Ni-MOF and Ni/Fe-MOF samples. Both samples show flake-like layers that make a 3D flower-like form in a smaller magnification. Ni/Fe-MOF has a broader thickness in the same magnification compared to Ni-MOF microspheres.

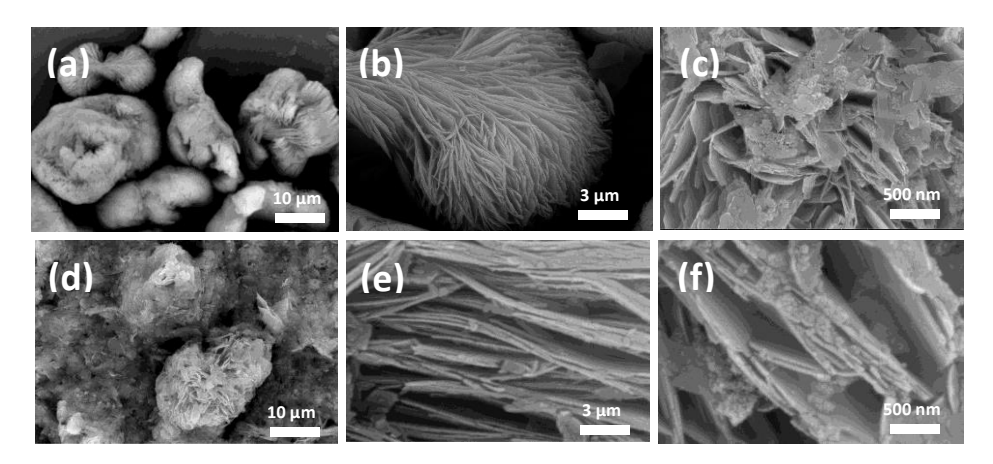


**Figure 2** SEM images of materials (a,b,c) Ni-MOF and (d,e,f) Ni/Fe-MOF at different magnifications.

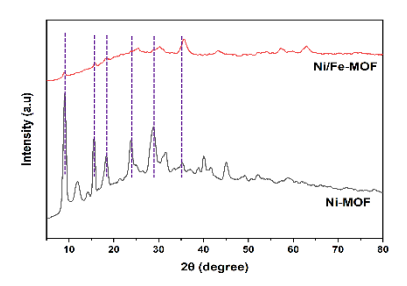
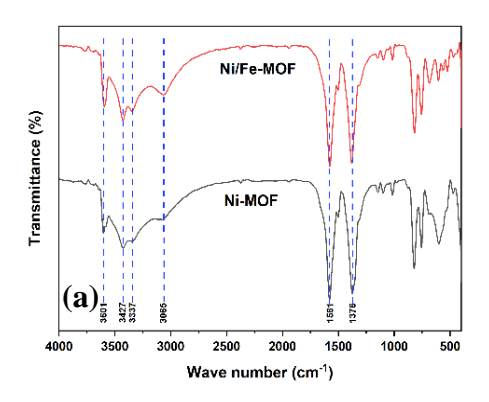
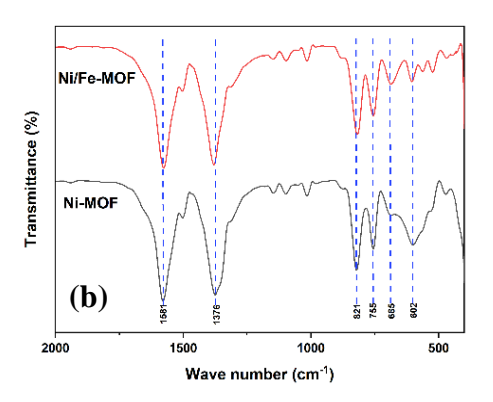


Figure 3 XRD pattern of Ni-MOF and Ni/Fe-MOF samples

Fig. 3 shows XRD patterns of Ni-MOF and Ni/Fe-MOF samples. Both of the samples show high amorphous components. The Ni-MOF peaks at around  $2\theta = 9.2^{\circ}$ ,  $11.8^{\circ}$ ,  $15.6^{\circ}$ ,  $18.36^{\circ}$ ,  $23.75^{\circ}$ ,  $28.76^{\circ}$ , and  $30.28^{\circ}$  corresponding to  $C_8H_6NiO_5 \cdot H_2O$  reported by Sherif, *et al* in [6]. Ni/Fe-MOF shows a slight shift to the right (higher angles) with lower peak intensity on  $2\theta$  between  $5^{\circ}$  and  $40^{\circ}$ . This indicates that Fe was successfully doped into Ni-MOF, corresponding to the previous literature on MOFs' substation, Wang, *et al* in [7].





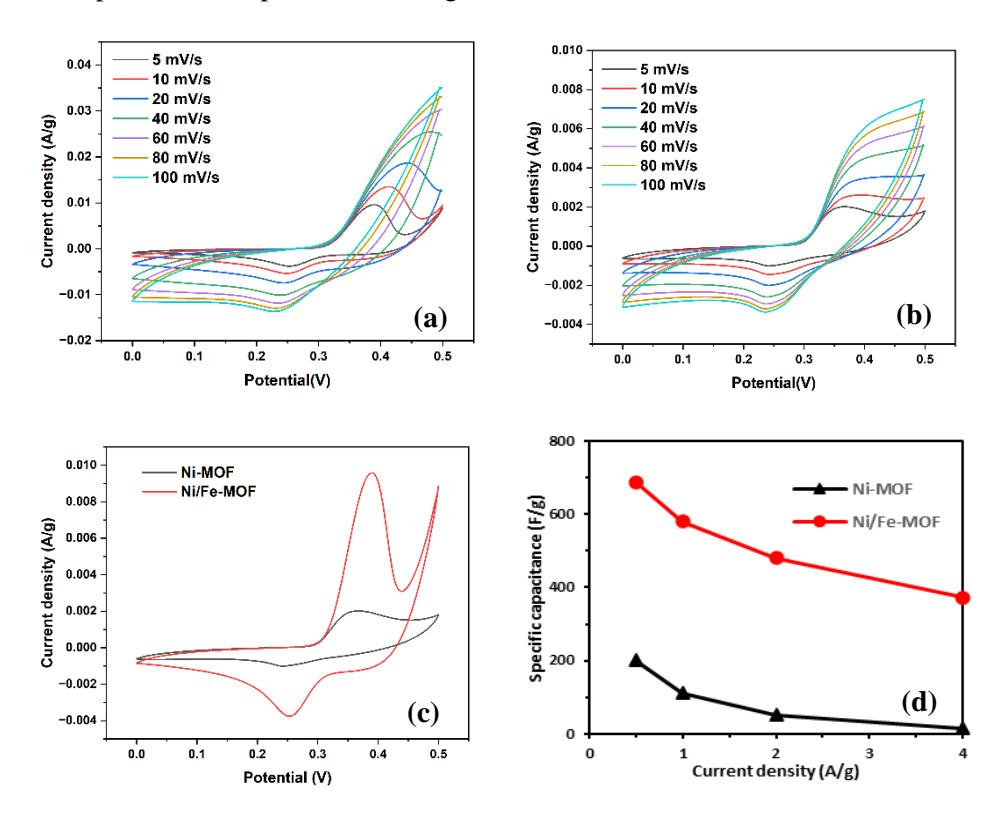
**Figure 4** FTIR spectrum result of Ni-MOF and Ni/Fe-MOF (a) 400-4000 cm<sup>-1</sup> (b) 400-2000 cm<sup>-1</sup>.

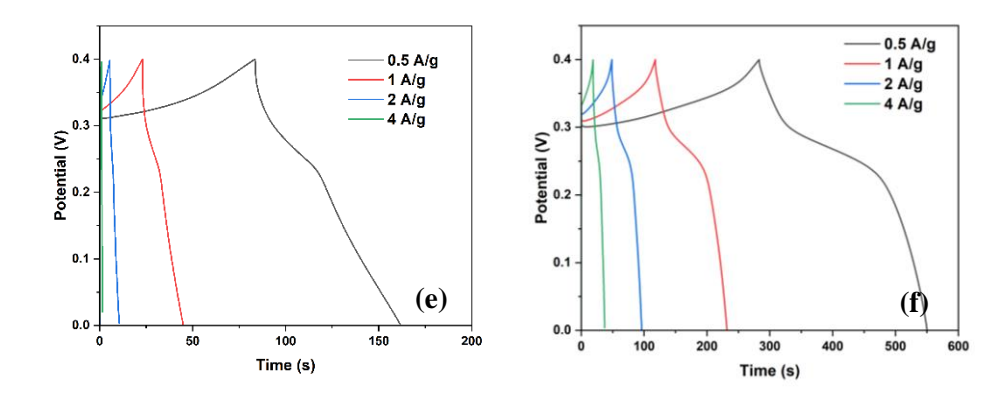
Most of the FTIR peaks in Fig. 4 are almost at the same wave number, further confirming that these frameworks are isostructural and have the same topology. Four distinct peaks at 3601, 3427, 3337, and 602 cm<sup>-1</sup> are attributed to the hydroxyl stretching vibrations of free water molecules (-OH), where the 602 cm<sup>-1</sup> peak represents an out-of-plane bending mode, Nandiyanto, *et al* in [8]. The absorption peaks 3065 cm<sup>-1</sup> are linked to the C-H bond, same with 821, 755, and 685 cm<sup>-1</sup> C-H, but have an out-of-plane bend [8]. Additionally, the prominent peaks at 1581 and 1376 cm<sup>-1</sup> are associated with the symmetric and asymmetric stretching vibrations of the carboxylate group (-COO), attributed to the Ni-COO-Ni and Fe-COO-Fe bonds, Chen, *et al* in [9]. The small absorption peak at 1144, 1097, and 1017 cm<sup>-1</sup> is assigned to the bending mode in the hydroxy-bridged complexes of the M-O-H vibration, as informed by Nakamoto, *et al* in [10].

 Table 1
 Specific surface area of samples.

Materials	Spesific surface area (m² g-¹)	Total pore per volume (cm <sup>2</sup> g <sup>-1</sup> )
Ni-MOF	16.976	0.181
Ni/Fe-MOF	78.693	0.5275

The specific surface area is presented in Table 1. Ni/Fe-MOF has a more specific surface area of 78.693 (m2 g<sup>-1</sup>) and a more total pore per volume of 0.5275 (cm2 g<sup>-1</sup>) than Ni-MOF. The high specific surface area is likely due to Fe incorporation into Ni-MOF altering the coordination environment of the metal sites, introducing a smaller average crystal size of 13.22 nm compared to pristine Ni-MOF, which has 23.69 nm. This can enhance porosity and create additional micropores or mesopores, increasing the surface area.





**Figure 5** (a) CV curves of Ni-MOF at a 5-100 mV s<sup>-1</sup> scan rate. (b) CV curves of Ni/Fe-MOF at a 5-100 mV s-1 scan rate. (c) CV curves of the Ni-MOF and Ni/Fe-MOF at 5 mV s<sup>-1</sup> scan rate. (d) Specific capacitance of Ni-MOF and Ni/Fe-MOF at various current densities. (e) GCD curves of Ni-MOF in different densities. (f) GCD curves of Ni/Fe-MOF in different densities.

Fig. 5a, 5 b, and 5c illustrate the cyclic voltammetry (CV) curves for Ni-MOF and Ni/Fe-MOF at different scan rates. The mean areas enclosed by the CV curves correspond to the specific capacities of the materials. Compared to Ni-MOF, Ni/Fe-MOF exhibits a larger area, signifying superior specific capacitance for the M-MOFs. The GCD curves in Fig. 5d, 5e, and 5f exhibit better specific capacitance for Ni/Fe-MOF, reaching 688 F g-1 more than Ni-MOF, with only 202 F g<sup>-1</sup> at 0.5 A g<sup>-1</sup> current density.

## 4 Conclusions

Bimetallic Ni/Fe-MOF has been successfully obtained by the solvothermal method with a ratio of 1:1. It has almost the same flake-like morphology as Ni-MOF but performs better. It delivers specific capacitance up to 688 F g<sup>-1</sup> at 0.5 A g<sup>-1</sup>. The improved performance can be credited to the increased specific surface area and higher pore density per unit volume. The high specific surface area is likely due to Fe incorporation into Ni-MOF alters the coordination environment of the metal sites, introducing a smaller average crystal size of 13.22 nm compared to pristine Ni-MOF, which has 23.69 nm. Therefore, this study can provide new insight into bimetallic Ni/Fe-MOF for supercapacitor electrode that positively affects electrochemical performance.

# Acknowledgment

This research was supported by Institut Teknologi Bandung and PT PLN (Persero). We thank the Advanced Functional Materials Laboratory for providing the materials and apparatus for this research, our colleagues from the Master Program of Engineering Physics PLN-ITB, and AFM Laboratory members for their assistance.

#### References

- [1] Q. Abbas, M. Mirzaeian, M. R. C. Hunt, P. Hall, and R. Raza, "Current State and Future Prospects for Electrochemical Energy Storage and Conversion Systems," *Energies*, vol. 13, no. 21, p. 5847, Nov. 2020. (Journal)
- [2] G. Navarro, J. Torres, M. Blanco, J. Nájera, M. Santos-Herran, and M. Lafoz, "Present and Future of Supercapacitor Technology Applied to Powertrains, Renewable Generation and Grid Connection Applications," *Energies*, vol. 14, no. 11, p. 3060, May 2021. (Journal)
- [3] A. Khan, "Metal-Organic Frameworks for Chemical Reactions," in *Metal-Organic Frameworks for Chemical Reactions*, Elsevier, 2020, pp. i–iii. (Book)
- [4] N. Raza, T. Kumar, V. Singh, and K.-H. Kim, "Recent advances in bimetallic metal-organic framework as a potential candidate for supercapacitor electrode material," *Coordination Chemistry Reviews*, vol. 430, p. 213660, Mar. 2021. (Journal)
- [5] Y. Nie *et al.*, "Incorporated ferrocene-derivatives endow Ni-based MOF with high-performance for electrochemical detection," *Colloids and Surfaces A: Physicochemical and Engineering Aspects*, vol. 680, p. 132742, Jan. 2024. (Journal)
- [6] F. G. Sherif, "Heavy Metal Terephthalates," *Product R&D*, vol. 9, no. 3, pp. 408–412, Sep. 1970. (Journal)
- [7] J. Wang, Q. Zhong, Y. Xiong, D. Cheng, Y. Zeng, and Y. Bu, "Fabrication of 3D Co-doped Ni-based MOF hierarchical micro-flowers as a high-performance electrode material for supercapacitors," *Applied Surface Science*, vol. 483, pp. 1158–1165, Jul. 2019. (Journal)
- [8] A. B. D. Nandiyanto, R. Ragadhita, and M. Fiandini, "Interpretation of Fourier Transform Infrared Spectra (FTIR): A Practical Approach in the Polymer/Plastic Thermal Decomposition," *Indonesian J. Sci. Technol*, vol. 8, no. 1, pp. 113–126, Sep. 2022. (Book)

- [9] H. Chen, Y. Huo, K. Cai, and Y. Teng, "Controllable preparation and capacitance performance of bimetal Co/Ni-MOF," *Synthetic Metals*, vol. 276, p. 116761, Jun. 2021. (Journal)
- [10] K. Nakamoto, *Infrared and Raman spectra of inorganic and coordination compounds. Part A: Theory and applications in inorganic chemistry*, 6. ed. Hoboken, NJ: Wiley, 2009. (Journal)